

# X-Ray Diffraction (XRD) and Surface Morphology Studies of PVC complexes Modified with Doping Salt and Additives

Siti Khatijah Deraman<sup>1</sup>, Nazrizawati Ahmad Tajuddin<sup>2</sup>, Hussein Hanibah<sup>1\*</sup>

<sup>1</sup>Centre of Foundation Studies, Universiti Teknologi MARA, Cawangan Selangor, Kampus Dengkil 43800 Dengkil, Selangor, Malaysia

<sup>2</sup>School of Chemistry and Environment, Faculty of Applied Sciences, Universiti Teknologi MARA (UiTM), 40450 Shah Alam, Selangor, Malaysia

## ARTICLE INFO

### Article history:

Received 1 October 2023

Revised 18 January 2024

Accepted 19 March 2024

Online first

Published 24 June 2024

### Keywords:

Polyvinyl Chloride (PVC)

X-ray diffraction

Surface Morphology

Polymer electrolytes

Amorphous

### DOI:

10.24191/sl.v18i2.22877

## ABSTRACT

In this work, the proton-conducting polymer electrolytes were prepared using the solution casting technique. Poly (vinyl chloride) PVC is used as the polymer host, ammonium triflate (NH<sub>4</sub>CF<sub>3</sub>SO<sub>3</sub>) as the doping salt, and ethylene carbonate (EC) and butyltrimethyl ammonium bis trifluoromethyl sulfonyl imide (Bu<sub>3</sub>MeNTf<sub>2</sub>N) is used as the plasticizers. XRD and FESEM characterization techniques were used to study the properties of the PVC-based proton-conducting polymer electrolytes. XRD studies show that amorphous PVC becomes largely amorphous upon adding NH<sub>4</sub>CF<sub>3</sub>SO<sub>3</sub>. Largely amorphous is also obtained upon adding EC and Bu<sub>3</sub>MeNTf<sub>2</sub>N to PVC-NH<sub>4</sub>CF<sub>3</sub>SO<sub>3</sub>. XRD studies of the salted samples showed they are largely amorphous. However, XRD studies could not identify the most amorphous sample for sure. Identifying the most amorphous sample is imperative, as conduction in polymer electrolytes is known to occur in the amorphous region. The FESEM micrographs gave a qualitative idea of the amorphousity of the salted samples in that 30 wt. % NH<sub>4</sub>CF<sub>3</sub>SO<sub>3</sub> (A4) had the greyest regions in its micrograph, giving a strong indication of it being the most amorphous sample. In the case of the EC plasticized system, the micrographs showed that the pore size increased with increasing concentration of EC, which in turn caused the amorphous regions (a grey area) to decrease. This means that 5 wt. % of EC (B1), which has the smallest pore size and the greyest area, is the most amorphous sample. In the micrographs of Bu<sub>3</sub>MeNTf<sub>2</sub>N plasticized samples, the sample 15 wt. % Bu<sub>3</sub>MeNTf<sub>2</sub>N (C3) is observed to be more homogeneous with whiter spherulites indicating the presence of more trapped ionic liquid. This indicates that 15 wt. % Bu<sub>3</sub>MeNTf<sub>2</sub>N (C3) is the most amorphous due to its homogeneity compared to the sample 5 wt. % Bu<sub>3</sub>MeNTf<sub>2</sub>N (C1). XRD results show that the salt and plasticizers have decreased the crystallinity of PVC and salted PVC-based polymer electrolytes. The surface morphology images give a qualitative idea of the degree of crystallinity of the complexes studied in this work.

## INTRODUCTION

Generally, polymers are known to be electrical insulators. These insulating materials, known as polymer electrolytes, can conduct electricity by introducing ions in their matrices. The first ion-conducting polymer electrolytes were discovered in 1973 [1]. This was followed by the practical application of an all-solid-state battery using ion-conducting polymer films in 1979 [2]. These novel discoveries motivated

\* Corresponding author. E-mail address: drsitikhatijah@uitm.edu.my

scientists from academic institutions and industrial sectors to pursue intensive research in materials science. Consequently, a large number of polymer electrolyte materials involving different types of transporting ions, namely  $\text{Li}^+$  [3],  $\text{Na}^+$  [4],  $\text{K}^+$  [5],  $\text{Cu}^+$  [6],  $\text{Ag}^+$  [7], and  $\text{H}^+$  [8] have been investigated since then. In this work, PVC is chosen as the polymer host since this material has been well-studied by various scientists due to its unique characteristics [9-14]. The use of PVC as a host is mainly because of the presence of lone pair electrons at the chlorine atom where inorganic salts can be complexed and also the dipole-dipole interaction between hydrogen and chlorine atoms, which can stiffen the polymer backbone [15, 16].

Most works reported on PVC-based polymer electrolytes are doped with lithium inorganic salts [17-20]. As such, in this work, PVC is used as a base for proton-conducting polymer electrolytes by adding  $\text{NH}_4\text{CF}_3\text{SO}_3$ , an ammonium-based inorganic salt. So far, several reports have been on PVC as a host for proton-conducting electrolyte systems. Thus, it will be interesting to investigate the properties of proton-conducting polymer electrolytes based on PVC to discover more of their properties. The prepared PVC- $\text{NH}_4\text{CF}_3\text{SO}_3$  polymer electrolyte system will be added with plasticizer EC, ionic liquid (IL), and  $\text{Bu}_3\text{MeNTf}_2\text{N}$  separately to compare the effects of these plasticizers.

Therefore, X-ray diffraction (XRD) patterns and surface morphology of pure PVC and the polymer electrolytes prepared in this work are presented. X-ray diffraction studies are carried out to compare the nature of crystallinity and the occurrence of complexation. In contrast, changes in surface morphology and structure of the polymer systems can be studied via field emission scanning electron microscopy. Only the X-ray diffraction pattern will be presented in the case of Ammonium Triflate ( $\text{NH}_4\text{CF}_3\text{SO}_3$ ). This is followed by the X-ray diffraction patterns and surface morphology image of the complexes PVC- $\text{NH}_4\text{CF}_3\text{SO}_3$ , PVC- $\text{NH}_4\text{CF}_3\text{SO}_3$ -EC, and PVC- $\text{NH}_4\text{CF}_3\text{SO}_3$ - $\text{Bu}_3\text{MeNTf}_2\text{N}$  due to Tetrahydrofuran (THF) evaporation. These diffractograms and micrographs are presented to study the effects of the addition of plasticizer / ionic liquid on the structure of the PVC-  $\text{NH}_4\text{CF}_3\text{SO}_3$  complexes.

## EXPERIMENTAL

The solution cast technique is used to prepare solid proton-conducting polymer electrolytes. In the present study, PVC is used as the polymer host. Three (3) different systems were prepared in which PVC- $\text{NH}_4\text{CF}_3\text{SO}_3$ , PVC- $\text{NH}_4\text{CF}_3\text{SO}_3$ -EC, and PVC- $\text{NH}_4\text{CF}_3\text{SO}_3$ - $\text{Bu}_3\text{MeNTf}_2\text{N}$  (Ionic Liquid) system. The section begins with the sample preparation technique and the compositions of the prepared polymer electrolyte. The samples have been characterized using X-ray diffraction (XRD) and Field Emission Scanning Electron Microscopy (FESEM) to investigate the structural and optical properties of the samples.

### Materials Preparation

All the polymer electrolytes in this study are prepared using the solution cast technique. PVC with molecular weight of  $2.33 \times 10^5 \text{ gmol}^{-1}$ ,  $\text{NH}_4\text{CF}_3\text{SO}_3$  (Sigma- Aldrich, 99.0 %), EC (Sigma- Aldrich, 98.0 %) and  $\text{Bu}_3\text{MeNTf}_2\text{N}$  (Butyltrimethyl ammonium bis (trifluoromethyl sulfonyl) imide) ionic liquid (Sigma- Aldrich, 98.0 %) were used in this research. All chemicals were used as received.

### Sample Preparation

Proton-conducting electrolyte films containing various weight ratios of polymer host, doping salt, and additives (plasticizer / ionic liquid) are prepared using the solution casting technique. One gram of PVC was dissolved in 50 ml of THF. The mixture is stirred continuously with a magnetic stirrer for several hours at room temperature until the PVC has completely dissolved. Different amounts of  $\text{NH}_4\text{CF}_3\text{SO}_3$  (10 wt. % - 50 wt. %) are added to the PVC solutions and stirred until the salt completely dissolves. The solutions are then poured into different glass petri dishes and allowed to dry at room temperature for several days to obtain free-standing films. The films formed are further dried in a vacuum oven at 313 K with a pressure

of 10-3 torr for 24 h. The free-standing films are then kept in a desiccator for further drying. The present study prepares five polymer-salt electrolyte systems with different weight percent (wt. %) ratios. Table 1 summarizes the concentration of PVC and  $\text{NH}_4\text{CF}_3\text{SO}_3$  in wt. % used to prepare the PVC- $\text{NH}_4\text{CF}_3\text{SO}_3$  system and their designation/sample name.

Table 1. Composition of PVC -  $\text{NH}_4\text{CF}_3\text{SO}_3$  Polymer Electrolytes

Sample Name	PVC (g)	PVC (wt. %)	$\text{NH}_4\text{CF}_3\text{SO}_3$ (g)	$\text{NH}_4\text{CF}_3\text{SO}_3$ (wt. %)
A1	1.0	1.0	0.0000	0.0
A2	1.0	0.9	0.1111	0.1
A3	1.0	0.8	0.2500	0.2
A4	1.0	0.7	0.4286	0.3
A5	1.0	0.6	0.6667	0.4
A6	1.0	0.5	1.0000	0.5

In order to investigate the effect of plasticizers on the PVC-salt samples, the highest conducting PVC-salt sample (A4) is added with two different plasticizers, which are ethylene carbonate (EC) and Bu3MeNTf2N (Butyltrimethyl ammonium bis (trifluoromethyl sulfonyl) imide). The preparation steps are similar to those used to prepare PVC-  $\text{NH}_4\text{CF}_3\text{SO}_3$  samples; in all these samples, the amount of PVC and salt are kept constant. Tables 2 and Table 3 list the composition of these samples together with their sample name.

Table 2. Composition of PVC- $\text{NH}_4\text{CF}_3\text{SO}_3$ -EC Polymer Electrolytes

Sample Name	PVC- $\text{NH}_4\text{CF}_3\text{SO}_3$ [A4] (g)	EC (g)	EC (wt. %)
B1	1.4286	0.0752	0.05
B2	1.4286	0.1587	0.10
B3	1.4286	0.2521	0.15
B4	1.4286	0.3572	0.20
B5	1.4286	0.4762	0.25

Table 3. Composition of PVC- $\text{NH}_4\text{CF}_3\text{SO}_3$ -Bu3MeNTf2N Polymer Electrolytes

Sample Name	PVC- $\text{NH}_4\text{CF}_3\text{SO}_3$ [A4] (g)	Bu3MeNTf2N (g)	Bu3MeNTf2N (wt. %)
C1	1.4286	0.0752	0.05
C2	1.4286	0.1587	0.10
C3	1.4286	0.2521	0.15
C4	1.4286	0.3572	0.20
C5	1.4286	0.4762	0.25

The XRD spectra of the proton-conducting polymer electrolyte films studied in this work are recorded using an X'pert Pro Analytical Diffractometer for Bragg angles ( $2\theta$ ) varying from  $5^\circ$  to  $90^\circ$ . In order to understand how the surface morphology of the proton-conducting polymer electrolyte film changes with doping of salt and plasticizers, field emission scanning electron microscopy of the polymer electrolyte films was taken. The structure and surface morphology of polymer electrolyte films are essential properties of polymer electrolytes since they give us a qualitative idea of the degree of crystallinity ( $X_c$ ) of polymer

films. In the present work, field emission scanning electron microscopy (FESEM) is carried out using FESEM, ZEISS SUPRATM 40VP at the Faculty of Applied Sciences, Universiti Teknologi MARA. The polymer electrolyte films were coated with a layer of platinum using Sputter Coater under a vacuum chamber with argon gas. The polymer electrolyte films were then attached to FESEM stubs using two-sided adhesive tape. The sample is examined at 5 kV for 500x, 3000x, and 10000x magnification to investigate the different spherulite sizes of the samples.

## RESULT AND DISCUSSION

### X-Ray Diffraction of PVC-NH<sub>4</sub>CF<sub>3</sub>SO<sub>3</sub> System

Figure 1.0 (a) illustrates the X-ray diffraction pattern of pure PVC (A1). The XRD spectrum of pure PVC lacks sharp peaks but is characterized by a broad peak from  $2\theta = 13$  to  $30^\circ$  with a center at  $25^\circ$ . The XRD pattern of pure PVC indicates that the sample has low crystallinity. The XRD pattern of pure PVC reported in this work is consistent with that reported by many studies [21-24].

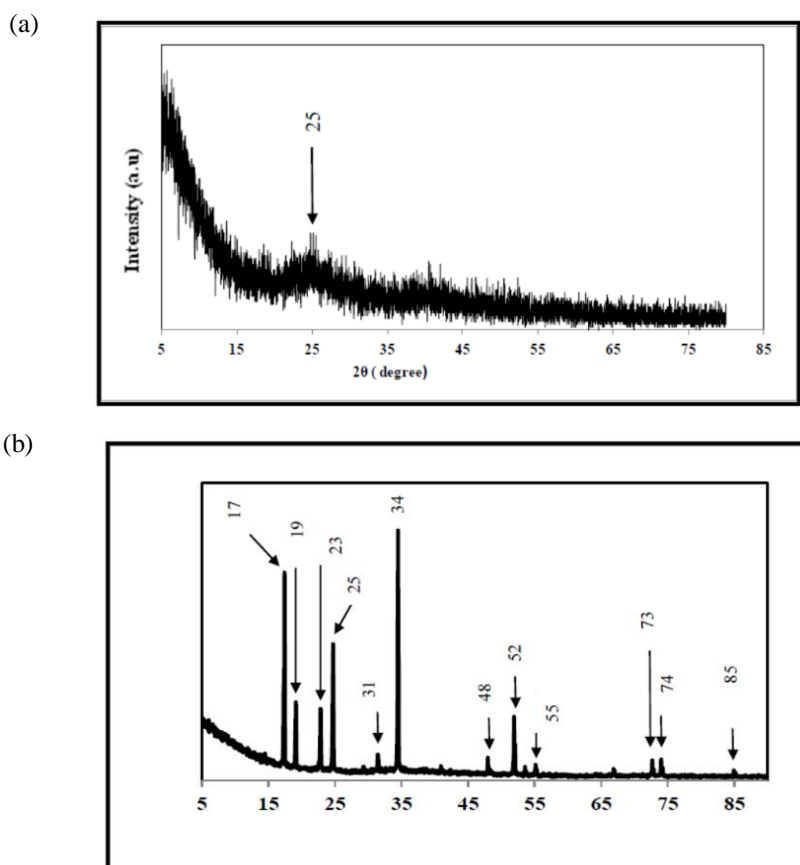


Fig. 1. XRD Spectrum of (a) Pure PVC (A1) and (b) Pure Ammonium Triflate

Figure 1(b) depicts the X-ray diffraction pattern of ammonium triflate (NH<sub>4</sub>CF<sub>3</sub>SO<sub>3</sub>) film. High intensity and well-distinguished peaks are observed in this spectrum at  $2\theta$  angles of 17, 19, 23, 25, 31, 34, 48, 52, 55, 73, 74, and  $85^\circ$ . By contrast to pure PVC, NH<sub>4</sub>CF<sub>3</sub>SO<sub>3</sub> is found to be crystalline in nature. The

XRD spectra of PVC -  $\text{NH}_4\text{CF}_3\text{SO}_3$  complexes for varying salt concentrations in wt. % are shown in Figure 2. The incorporation of the salt into polymeric PVC matrices displays the disappearance of the diffraction peaks of the salt at all  $2\theta$  angles of 17, 19, 23, 25, 31, 34, 48, 52, 55, 73, 74, and  $85^\circ$ . Since no peaks corresponding to  $\text{NH}_4\text{CF}_3\text{SO}_3$  are observed in the complexes of PVC-  $\text{NH}_4\text{CF}_3\text{SO}_3$ , this indicates the absence of excess salt (uncomplexed) in the material [25-27]. It can be inferred from the diffractograms that the samples are mainly amorphous in nature as a broad peak hump is observed at  $2\theta$  angles between  $13^\circ$  to  $30^\circ$  with centers that shifted to lower  $2\theta$  values as the concentration of salt increases. Changes in the intensity of the broad peak may also be observed, with sample A4 (Figure 2 (a)) having a higher intensity (40 %) than the rest. Changes in the XRD pattern of PVC-  $\text{NH}_4\text{CF}_3\text{SO}_3$  systems observed here may affect the electrical conductivity of the samples. Several studies have reported that ionic conduction in polymer electrolytes occurs in the amorphous region [28-31].

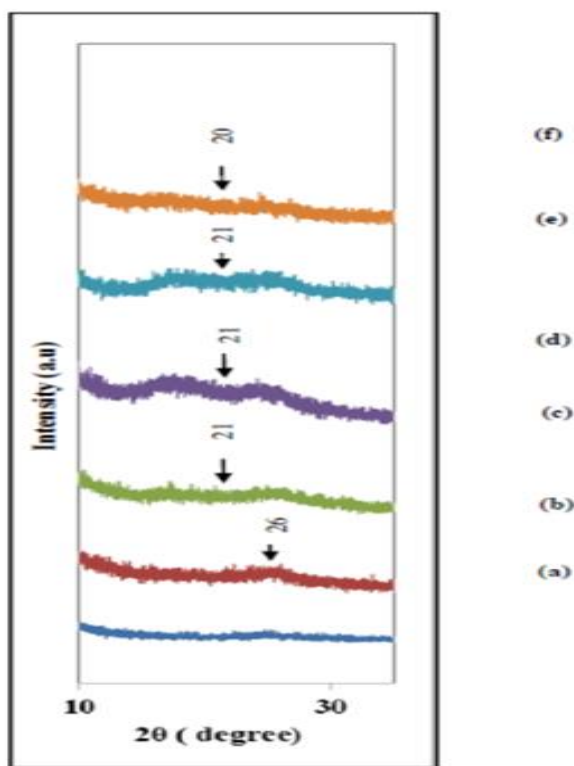


Fig. 2. XRD Spectra of (a) Pure PVC (A1) and PVC -  $\text{NH}_4\text{CF}_3\text{SO}_3$  Systems for Samples (b) A2 (c) A3 (d) A4 (e) A5 and (f) A6

### X-Ray Diffraction of PVC- $\text{NH}_4\text{CF}_3\text{SO}_3$ -EC System

Figure 3 shows the X-ray diffractograms of PVC-  $\text{NH}_4\text{CF}_3\text{SO}_3$ -EC complexes with various EC content in wt. %. When 5 wt. % of EC (B1) is added to PVC-  $\text{NH}_4\text{CF}_3\text{SO}_3$ , the diffraction pattern is characterized by a broad hump centered at  $2\theta = 23^\circ$ . As the concentration of EC increases to 10 wt. % (B2), the center of the hump shifted to  $21^\circ$ . The relative intensity of the hump is also observed to be higher at 5 wt. % (B1) plasticizer concentration.

In addition, when the EC concentration is 15 wt. % (B3), the center of the hump shifted to  $18^\circ$  while its relative intensity decreased. Beyond 20 wt. % EC (B4) concentration, the relative intensity of the halo increased again. This shows that adding EC changes the degree of crystallinity of the PVC-  $\text{NH}_4\text{CF}_3\text{SO}_3$ -EC system. The presence of the halo or amorphous hump in the diffraction patterns of PVC-  $\text{NH}_4\text{CF}_3\text{SO}_3$ -EC complexes implies that the samples are mainly amorphous in nature, while the increase in the intensity of the halo beyond 20 wt. % EC (B4) indicates that the crystallinity of the complexes increased again.

In short, the sample with 5 wt. % EC (B1) is the most amorphous. In other words, adding EC reduces the material's crystallinity, which is attributed to the interaction between the polymer and the plasticizer. The plasticizer may have disrupted the original polymer structure, manifested by the broad peak centered at  $2\theta = 23^\circ$ . The disordered arrangement of the polymer matrix occurs with the incorporation of EC, leading to the construction of an amorphous region. This aids in enhancing the segmental motion and flexibility of the polymer backbone. Hence, it results in an increment of ionic transportation due to higher ionic conductivity. Such shifts and changes in intensity indicate that complexation has occurred, as reported by several studies [32-37]. This implies that the plasticizer may have disrupted the host polymer's structure, forming smaller crystallite sizes. Therefore, adding the plasticizer EC can reduce the crystalline phase of the PVC films and increase the fraction of the amorphous region.

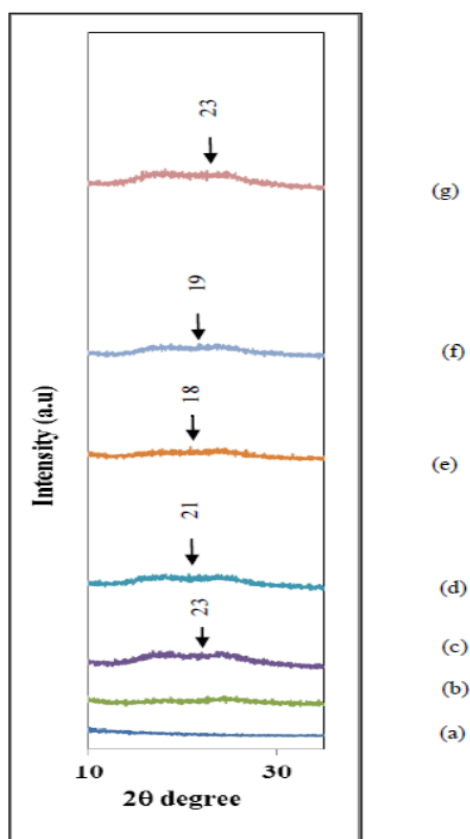


Fig. 3. XRD Spectra of (a) Pure PVC (A1), (b) PVC - 30 wt. %  $\text{NH}_4\text{CF}_3\text{SO}_3$  (A4) and PVC -  $\text{NH}_4\text{CF}_3\text{SO}_3$  -EC Systems for Samples (c) B1 (d) B2 (e) B3 (f) B4 and (g) B5

### X-Ray Diffraction of PVC-NH<sub>4</sub>CF<sub>3</sub>SO<sub>3</sub>-Bu<sub>3</sub>MeNTf<sub>2</sub>N System

Figure 4 depicts the XRD spectra of PVC-NH<sub>4</sub>CF<sub>3</sub>SO<sub>3</sub>-Bu<sub>3</sub>MeNTf<sub>2</sub>N complexes. As in the previous study, salt and PVC in all the films were kept constant. It is observed that the XRD spectra of the Bu<sub>3</sub>MeNTf<sub>2</sub>N plasticized system are characterized by a broad hump centered at  $2\theta = 19^\circ$  for 5 wt. % Bu<sub>3</sub>MeNTf<sub>2</sub>N (C1) concentration. This is a shift to a lower  $2\theta$  value when compared to A4. The shift in values  $2\theta$  upon the incorporation of Bu<sub>3</sub>MeNTf<sub>2</sub>N indicates that complexation between polymer and Bu<sub>3</sub>MeNTf<sub>2</sub>N has occurred [38, 39]. As the concentration of ionic liquid added is increased beyond 5 wt. %, the centre of the hump shifted from  $19^\circ$  (5 wt. % Bu<sub>3</sub>MeNTf<sub>2</sub>N) to higher  $2\theta$  values at  $21^\circ$  and  $22^\circ$  for Bu<sub>3</sub>MeNTf<sub>2</sub>N concentration of 15 wt. % (C3) and 20 wt. % (C4) respectively. Besides the shifting of the center of the hump to the lower  $2\theta$  values at  $20^\circ$ , the relative intensity of the center of the hump decreases for Bu<sub>3</sub>MeNTf<sub>2</sub>N concentration beyond 10 wt. % (C2).

The changes in the  $2\theta$  position of the center of the hump, as well as changes in the value of its relative intensity, indicate that possible complex formation between PVC, NH<sub>4</sub>CF<sub>3</sub>SO<sub>3</sub>, and Bu<sub>3</sub>MeNTf<sub>2</sub>N has taken place. The presence of the amorphous hump indicates that the PVC- NH<sub>4</sub>CF<sub>3</sub>SO<sub>3</sub>-Bu<sub>3</sub>MeNTf<sub>2</sub>N complexes are mainly amorphous in nature. This implies that the plasticizer may have disrupted the host polymer's structure, forming smaller crystallite sizes. It follows, therefore, that the addition of the ionic liquid, Bu<sub>3</sub>MeNTf<sub>2</sub>N, can reduce the crystalline phase of the PVC films and increase the fraction of the amorphous region. In other words, the role of Bu<sub>3</sub>MeNTf<sub>2</sub>N is much like that of EC reported earlier. Adding these plasticizers causes an increase in the degree of amorphousness of the PVC-based electrolytes.

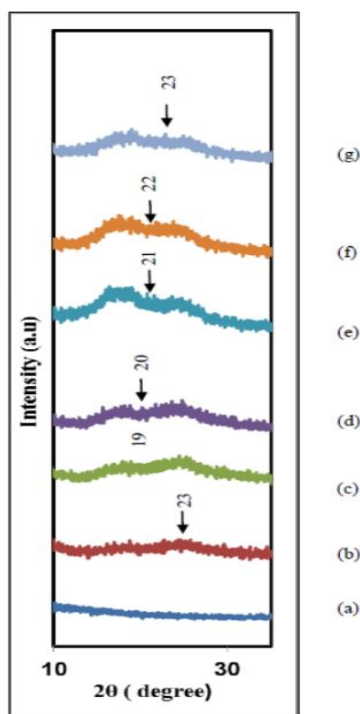


Fig. 4. XRD Spectra of (a) Pure PVC (A1) (b) PVC - 30 wt. % NH<sub>4</sub>CF<sub>3</sub>SO<sub>3</sub> (A4), PVC - NH<sub>4</sub>CF<sub>3</sub>SO<sub>3</sub> - Bu<sub>3</sub>MeNTf<sub>2</sub>N Systems for Samples (c) C1 (d) C2 (e) C3 (f) C4 and (g) C5

### FESEM Micrographs of PVC- NH<sub>4</sub>CF<sub>3</sub>SO<sub>3</sub> System

Figure 5 (a)-(d) presents the surface morphology of pure PVC (A1), PVC-10 wt. % NH<sub>4</sub>CF<sub>3</sub>SO<sub>3</sub> (A2), PVC-30 wt. % NH<sub>4</sub>CF<sub>3</sub>SO<sub>3</sub> (A4) and PVC-50 wt. % NH<sub>4</sub>CF<sub>3</sub>SO<sub>3</sub> (A6) at 500 × magnification. The FESEM images of PVC show the presence of some craters, which are spherical with a size of about 10-20 μm. This is consistent with the work reported by Ramesh *et al.* [40] and El-Naggar *et al.* [41]. The rapid volatilization of THF solvent during preparation contributes to this phenomenon [42, 43]. Upon incorporation of NH<sub>4</sub>CF<sub>3</sub>SO<sub>3</sub>, the pore size decreased to 5 μm. A similar decrease in pore size was also reported by Anuar *et al.* (2012) when NH<sub>4</sub>CF<sub>3</sub>SO<sub>3</sub> was incorporated into PEMA. It is also observed that the film with 30 wt. % NH<sub>4</sub>CF<sub>3</sub>SO<sub>3</sub> (A4) has a higher amorphous region, as indicated by the grey-colored regions in the micrographs. In contrast, the morphology of PVC-NH<sub>4</sub>CF<sub>3</sub>SO<sub>3</sub> with 50 wt. % NH<sub>4</sub>CF<sub>3</sub>SO<sub>3</sub> (A6) is seen to be more homogeneous with further reduction in pore size to 4 μm with fewer grey-colored areas, indicating that it is less amorphous. The decrease in pore size indicates that the salt has disrupted the morphology of PVC, resulting in structural reorganization of the polymer chain that may lead to H<sup>+</sup> ion transportation in the polymer matrix [20, 44].

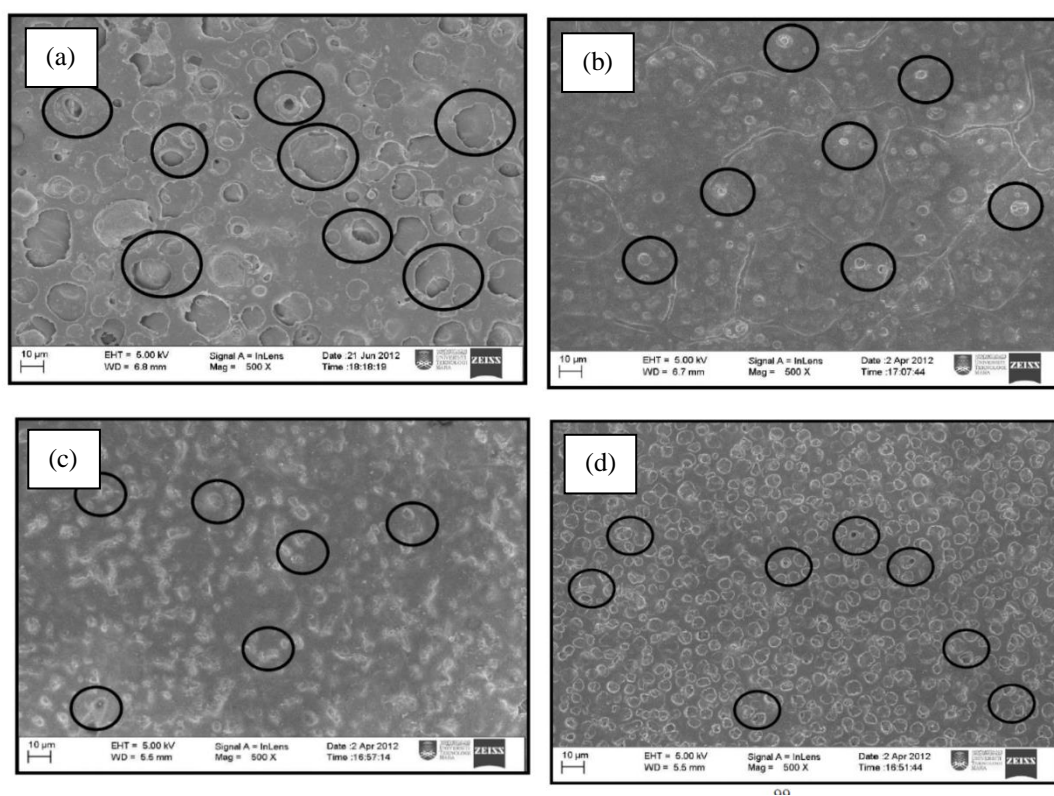


Fig. 5. Surface Morphology of (a) Pure PVC (A1) Film (b) PVC- NH<sub>4</sub>CF<sub>3</sub>SO<sub>3</sub> with 10 wt. % NH<sub>4</sub>CF<sub>3</sub>SO<sub>3</sub> (A2) (c) PVC- NH<sub>4</sub>CF<sub>3</sub>SO<sub>3</sub> with 30 wt. % NH<sub>4</sub>CF<sub>3</sub>SO<sub>3</sub> (A4) (d) PVC- NH<sub>4</sub>CF<sub>3</sub>SO<sub>3</sub> with 50 wt. % NH<sub>4</sub>CF<sub>3</sub>SO<sub>3</sub> (A6) at 500 × Magnification



**FESEM Micrographs of PVC-NH<sub>4</sub>CF<sub>3</sub>SO<sub>3</sub>-EC System**

Figure 6 (a)-(c) presents the surface morphology of PVC-NH<sub>4</sub>CF<sub>3</sub>SO<sub>3</sub>-EC at various concentrations at 500 × magnification. When 5 wt. % EC (B1) is complexed with PVC-NH<sub>4</sub>CF<sub>3</sub>SO<sub>3</sub>, the pore increased in size from 4 μm (PVC-NH<sub>4</sub>CF<sub>3</sub>SO<sub>3</sub>) to about 8 μm with some of them becoming more rectangular than spherical. The increase in pore size could be due to the presence of the plasticizer. This shows that the addition of EC has disrupted the morphology of the PVC- NH<sub>4</sub>CF<sub>3</sub>SO<sub>3</sub> complexes. Beyond 5 wt. % EC (B1), as the concentration of EC increases to 15 wt. % EC (B3), the pore size increases further to 10 μm, reducing the amorphous region between the pores. This means sample B1 is more amorphous than samples B3 and B5. This is consistent with the result from XRD discussed earlier. The pores in the micrographs indicate the occurrence of phase separation in the polymer electrolytes. The pores or craters formed on the surface are due to the rapid evaporation of the solvent (THF). The difference in the pore size is related to the difference in the driving force for phase separation [45, 46].

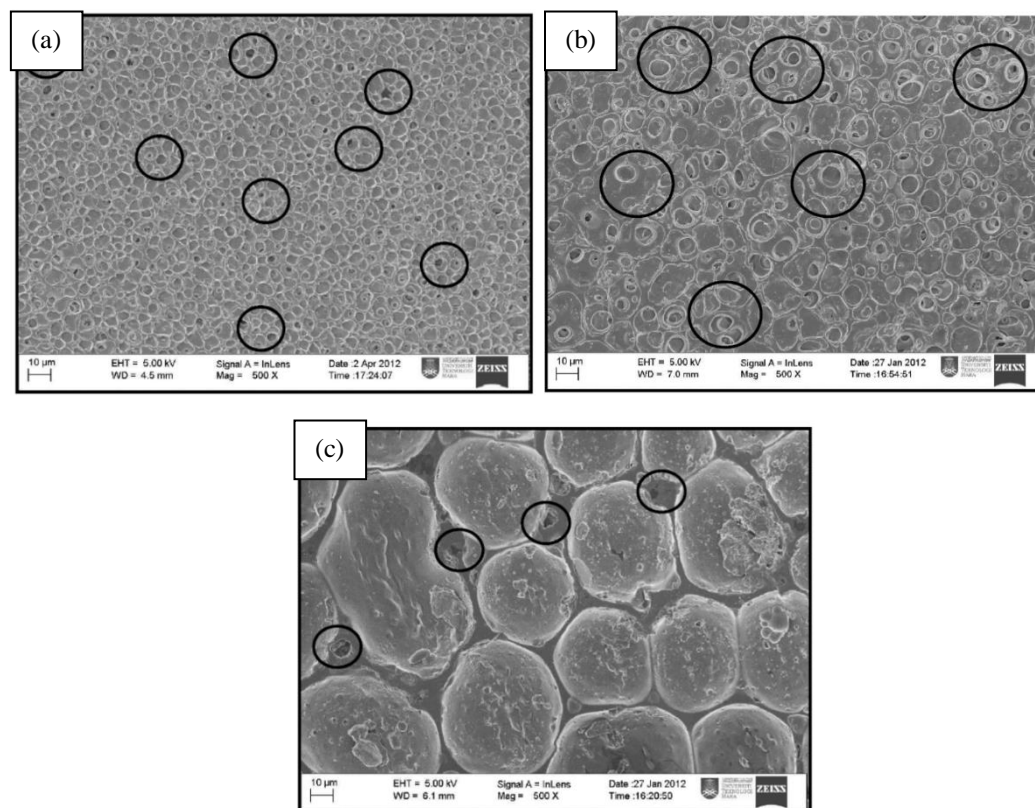


Fig. 6. Surface Morphology of PVC- NH<sub>4</sub>CF<sub>3</sub>SO<sub>3</sub>-EC with (a) 5 wt. % EC (B1) (b) 15 wt. % EC (B3) and (c) 25 wt. % EC (B5) at 500 × Magnification

### FESEM Micrographs of PVC- $\text{NH}_4\text{CF}_3\text{SO}_3$ - $\text{Bu}_3\text{MeNTf}_2\text{N}$ System

Figure 7 (a)-(b) presents the surface morphology of PVC-  $\text{NH}_4\text{CF}_3\text{SO}_3$ -  $\text{Bu}_3\text{MeNTf}_2\text{N}$  electrolytes with 5 wt. % (C1) and 15 wt. %  $\text{Bu}_3\text{MeNTf}_2\text{N}$  (C3) at  $500\times$  magnification. It can be noted that sample C1 is highly packed with small spheres, with some spheres embedded with small pores. These spheres represent the crystalline region of several platelets or lamellae radiating from a nucleating center called spherulites [31, 47]. The regions between the neighboring lamellae show the existence of an amorphous phase involved in ion conduction. The pore size is reduced to  $3\ \mu\text{m}$  when compared to the ionic liquid-free sample with smooth regions, suggesting the largely amorphous nature of the electrolyte. The presence of spherulites in the micrographs is mainly attributed to the entrapments of ionic liquid, which are retained in the polymer matrix. This induces the formation of the entanglements between ionic liquid and polymer network. These entanglements may enhance the segmental motion of the polymer backbone by weakening the interaction between polymer chains and  $\text{NH}_4^+$  cations. Thus, this produces a flexible polymer backbone and facilitates ionic transfer among the polymer network.

The amount of entrapments increases with increasing  $\text{Bu}_3\text{MeNTf}_2\text{N}$  loadings, as depicted in Figures 7 (a) and (b). The least entrapment in PVC-  $\text{NH}_4\text{CF}_3\text{SO}_3$ -5 wt. %  $\text{Bu}_3\text{MeNTf}_2\text{N}$  (C1) implies the least amorphous degree of the polymer matrix. The sample containing PVC-  $\text{NH}_4\text{CF}_3\text{SO}_3$ -15 wt. %  $\text{Bu}_3\text{MeNTf}_2\text{N}$  (C3) has more distribution of ionic liquid entrapments and tends to aggregate when compared to PVC-  $\text{NH}_4\text{CF}_3\text{SO}_3$ -5 wt. %  $\text{Bu}_3\text{MeNTf}_2\text{N}$  (C1). These aggregations weaken the coordination bonds of the polymer matrix and  $\text{NH}_4^+$  cations to form a more flexible polymer backbone with an enhanced plasticizing effect. Therefore,  $\text{Bu}_3\text{MeNTf}_2\text{N}$  interacts weakly with the polymer and salt, suggesting its lubricating action. This condition favors the ionic hopping mechanism, which should produce higher ionic conductivity. Some blackish cavities are formed on the surface morphology of PVC- $\text{NH}_4\text{CF}_3\text{SO}_3$ -15 wt. %  $\text{Bu}_3\text{MeNTf}_2\text{N}$  (C3), as highlighted in Figures 7 (a) and (b), discloses that there is interaction between  $\text{Bu}_3\text{MeNTf}_2\text{N}$  and components of the polymer electrolyte. This suggests the ionic migration effect by providing a continuous conducting pathway within the entrapments.

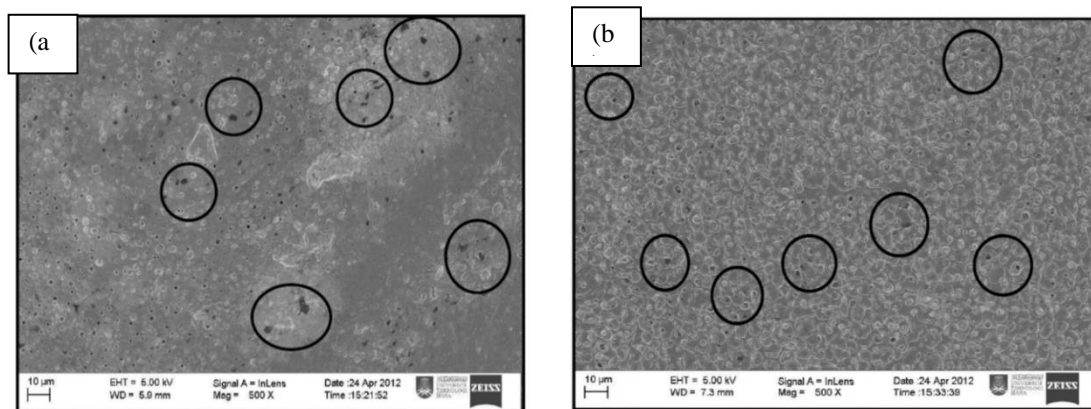


Fig.7. Surface Morphology of PVC-  $\text{NH}_4\text{CF}_3\text{SO}_3$ -  $\text{Bu}_3\text{MeNTf}_2\text{N}$  with (a) 5 wt. %  $\text{Bu}_3\text{MeNTf}_2\text{N}$  (C1) and (b) 15 wt. %  $\text{Bu}_3\text{MeNTf}_2\text{N}$  (C3) at  $500\times$  Magnification

## CONCLUSION

XRD results show that the salt and plasticizers have decreased the crystallinity of PVC and salted PVC-based polymer electrolytes. The complexation between the salt, plasticizers, and PVC occurs in the amorphous phase due to the decrease in the crystalline regions of the complexes. The surface morphology images give a qualitative idea of the degree of crystallinity of the complexes studied in this work. The surface morphology of the polymer electrolytes provides information on the structure of the materials studied, which XRD could not.

## ACKNOWLEDGEMENTS/FUNDING

The support from the Ministry of Education, Malaysia for Fundamental Research Grant Scheme-RACER (600-IRMI/FRGS-RACER 5/3 (123/2019)) is gratefully acknowledged.

## CONFLICT OF INTEREST STATEMENT

The authors declare that there are no conflicts of interest regarding the publication of this manuscript.

## AUTHORS' CONTRIBUTIONS

All authors contributed to the study equally.

## REFERENCES

- [1] Fenton, D. E., Parker, J. M., & Wright, P. V. (1973). Complexes of alkali metal ions with poly (ethylene oxide). *Polymer*, 14(11), 589.
- [2] Armand, M. B., Chabagno, J. M., & Duclot, M. J. (1979). In *fast ion transport in solids*, (P., Vashishta, J.N., Mundy, G. K., Shenoy, Eds) North Holland, New York: Elsevier.
- [3] Chew, S. Y., Sun, J., Wang, J., Liu, H., Forsyth, M., & MacFarlane, D. R. (2008). Lithium-polymer battery based on an ionic liquid-polymer electrolyte composite for room temperature applications. *Electrochimica acta*, 53(22), 6460-6463.
- [4] Sasikala, U., Kumar, P. N., Rao, V. V. R. N., & Sharma, A. K. (2012) Structural, electrical and parametric studies of a peo based polymer electrolyte for battery applications. *International Journal Of Engineering Science & Advanced Technology*, 2 (3), 722 – 730.
- [5] Lewandowski, A., Skorupska, K., & Malinska, J. (2000). Novel poly(vinyl alcohol)-KOH-H<sub>2</sub>O alkaline polymer electrolyte. *Solid State Ionics*, 133(3), 265-271.
- [6] Mani, P., Srivastava, R., & Strasser, P. (2011). Dealloyed binary PtM<sub>3</sub> (M = Cu, Co, Ni) and ternary PtNi<sub>3</sub>M (M = Cu, Co, Fe, Cr) electrocatalysts for the oxygen reduction reaction: Performance in polymer electrolyte membrane fuel cells. *Journal of Power Sources*, 196(2), 666-673.
- [7] Hirankumar, G., Selvasekarapandian, S., Kuwata, N., Kawamura, J., Hattori, T. (2005). Thermal, electrical and optical studies on the poly (vinyl alcohol) based polymer electrolytes, *Journal of Power Sources*, 144, 262-267.

- [8] Noda, A., Susan, M. A. B. H., Kudo, K., Mitsushima, S., Hayamizu, K., & Watanabe, M. (2003). Brønsted acid-base ionic liquids as proton-conducting nonaqueous electrolytes. *The Journal of Physical Chemistry B*, 107(17), 4024-4033.
- [9] Ramesh, S., & Yi, L. J. (2008). FTIR spectra of plasticized high molecular weight PVC–LiCF<sub>3</sub>SO<sub>3</sub> electrolytes. *Ionics*, 15(4), 413–420.
- [10] Elizabeth, R. N., Saito, Y., & Stephan, A. M. (2004). Preparation and Characterization of PVC / PMMA Blend Polymer Electrolytes Complexed with LiN(C<sub>2</sub>F<sub>5</sub>SO<sub>2</sub>)<sub>2</sub>, 14, 1–7.
- [11] Choi, N. S., & Park, J. K. (2001). New polymer electrolytes based on PVC/PMMA blend for plastic lithium-ion batteries. *Electrochimica acta*, 46(10), 1453-1459.
- [12] Subban, R. H. Y., & Arof, A. K. (2003). Experimental Investigations on PVC–LiCF<sub>3</sub>SO<sub>3</sub>- 309 SiO<sub>2</sub> Composite Polymer Electrolytes. *Journal of New Materials for Electrochemical Systems* 6, 197–203.
- [13] Kulasekarapandian, K., Jayanthi, S., Muthukumari, A., Arulsankar, A., & Sundaresan, B. (2013). Preparation and Characterization of PVC–PEO Based Polymer Blend Electrolytes Complexed With Lithium Perchlorate. *International Journal of Engineering Research and Development*, 5 (11), 30-39.
- [14] Kumari, N., Mohan, C., & Negi, A. (2023). An investigative study on the structural, thermal, and mechanical properties of clay-based PVC polymer composite films. *Polymers*, 15(8), 1922.
- [15] Uma, T., Mahalingam, T., & Stimming, U. (2005). Conductivity studies on poly(methyl methacrylate)–Li<sub>2</sub>SO<sub>4</sub> polymer electrolyte systems. *Materials chemistry and physics*, 90(2), 245-249.
- [16] El-Naggar, A. M., Heiba, Z. K., Kamal, A. M., Abd-Elkader, O. H., & Mohamed, M. B. (2023). Impact of ZnS/Mn on the structure, optical, and electric properties of PVC polymer. *Polymers*, 15(9), 2091
- [17] Rajendran, S., & Uma, T. (2000). Effect of ZrO<sub>2</sub> on conductivity of PVC-PMMA-LiBF<sub>4</sub>- DBP polymer electrolytes. *Bulletin of Materials Science*, 23(1), 31-34
- [18] Rajendran, S., Song, M. S., Park, M. S., Kim, J. H., & Lee, J. Y. (2005). Lithium ion conduction in PVC–LiN(CF<sub>3</sub>SO<sub>2</sub>)<sub>2</sub> electrolytes gelled with PVdF. *Materials Letters*, 59(18), 2347–2351.
- [19] Vickraman, P., Aravindan, V., Selvambikai, M., & Shankarasubramanian, N. (2009). Ionic transport, thermal, XRD, and phase morphological studies on LiCF<sub>3</sub>SO<sub>3</sub>- based PVC–PVdF gel electrolytes. *Ionics*, 15(4), 433-437
- [20] Alshammari, A. H., Alshammari, M., Alshammari, K., Allam, N. K., & Taha, T. A. (2023). PVC/PVP/SrTiO<sub>3</sub> polymer blend nanocomposites as potential materials for optoelectronic applications. *Results in Physics*, 44, 106173.
- [21] Stephan, A. M., Thirunakaran, R., Renganathan, N. G., Sundaram, V., Pitchumani, S., 308 Muniyandi, N., Gangadharan R. & Ramamoorthy, P. (1999). A study on polymer blend electrolyte based on PVC/PMMA with lithium salt. *Journal of power sources*, 81, 752-758.
- [22] Rajendran, S., Uma, T. & Mahalingam T. (2000). Conductivity studies on PVC±PMMA±LiAsF<sub>6</sub>±DBP polymer blend electrolyte. *European Polymer Journal*, 36, 2617–2620.
- [23] Rajendran, S. and Uma, T. (2000b). Lithium ion conduction in PVC-LiBF<sub>4</sub> electrolytes gelled with PMMA. *Journal of Power Sources*, 88, 282– 285.
- [24] Barkhordari, A., Altindal, Ş., Pirgholi-Givi, G., Mashayekhi, H., Özçelik, S., & Azizian-Kalandaragh, Y. (2023). The influence of PVC and (PVC: SnS) interfacial polymer layers on the electric and dielectric properties of Au/n-Si structure. *Silicon*, 15(2), 855-865.
- [25] Rajendran, S., Uma, T. & Mahalingam T. (2000). Conductivity studies on PVC±PMMA±LiAsF<sub>6</sub>±DBP polymer blend electrolyte. *European Polymer Journal*, 36, 2617–2620.

- [26] Rajendran, S. and Uma, T. (2000b). Lithium ion conduction in PVC-LiBF<sub>4</sub> electrolytes gelled with PMMA. *Journal of Power Sources*, 88, 282–285
- [27] Khaleghi, M. (2022). Experimental and computational study of thermal behavior of PVC composites based on modified eggshell biofiller for UPVC product. *Journal of Polymer Research*, 29(1), 2.
- [28] Srivastava, N., Chandra, A., Chandra, S. (1995) Dense branched growth of (SCN)<sub>x</sub> and ion transport in the poly (ethylene oxide) NH<sub>4</sub>SCN polymer electrolyte, *Physical Review B* 52, 225-230.
- [29] Maurya, K.K., Hashmi, S.A., Chandra, S. (1992a) Proton conducting polymer electrolytes: polyethylene oxide + (NH<sub>4</sub>)<sub>2</sub>SO<sub>4</sub> system, *Journal of the Physical Society of Japan* 61, 1709-1716.
- [30] Mohamed, N.S., Zakaria, M.Z., Ali, A.M.M. & Arof, A.K. (1997). Characteristics of poly(ethylene oxide)- NaI polymer electrolyte and electrochemical cell performance. *Journal of Power Sources* 66:169-172.
- [31] Kassem, S. M., Abdel Maksoud, M. I. A., El Sayed, A. M., Ebraheem, S., Helal, A. I., & Ebaid, Y. Y. (2023). Optical and radiation shielding properties of PVC/BiVO<sub>4</sub> nanocomposite. *Scientific Reports*, 13(1), 10964.
- [32] Hashmi, S.A., Kumar, A., Maurya, K.K., Chandra, S. (1990) Proton-conducting polymer electrolyte II. The polyethylene oxide + NH<sub>4</sub>ClO<sub>4</sub> system, *Journal of Physics D: Applied Physics* 23, 1307-1314.
- [33] Sekhon S. S., Singh G., Agnihotry S. A., Chandra S. (1995) Solid polymer electrolytes based on polyethylene oxide-silver thiocyanate, *Solid state Ionics* 80, 37-44
- [34] Acosta, J.L., Morales, E. (1996) Structural, morphological and electrical characterization of polymer electrolytes based on PEO/PPO blends, *Solid State Ionics* 85, 85-90
- [35] Gupta, P.N & Singh, K.P. (1996) Characterization of H<sub>2</sub>PO<sub>4</sub> Based PVA complex system, *Solid State Ionics*, 86-88 (1), 319-323
- [36] Kim, J.Y and Kim, S.H., (1999) Ionic conduction behavior of network polymer electrolytes based on phosphate and Polyether copolymers, *Solid State Ionics*, 124, 91-99.
- [37] Ouyang, Z., Li, S., Zhao, M., Wangmu, Q., Ding, R., Xiao, C., & Guo, X. (2022). The aging behavior of polyvinyl chloride microplastics promoted by UV-activated persulfate process. *Journal of Hazardous Materials*, 424, 127461.
- [38] Noor, S. A. M., Ahmad, A., Talib, I. A., & Rahman, M. Y. A. (2010). Morphology, chemical interaction, and conductivity of a PEO-ENR50 based on solid polymer electrolyte. *Ionics*, 16 (2), 161-170.
- [39] Konwar, S., Singh, P. K., Dhapola, P., Singh, A., Savirov, S. V., Yahya, M. Z. A., ... & Gultekin, B. (2023). Developing Biopolymer-Based Electrolytes for Supercapacitor and Dye-Sensitized Solar Cell Applications. *ACS Applied Electronic Materials*, 5(10), 5503-5512.
- [40] Ramesh, S., Winie, T., & Arof, A. K. (2010). Mechanical studies on poly (vinyl chloride)-poly (methyl methacrylate)-based polymer electrolytes. *Journal of materials science*, 45(5), 1280-1283.
- [41] El-Naggar, A. M., Heiba, Z. K., Kamal, A. M., Abd-Elkader, O. H., & Mohamed, M. B. (2023). Impact of ZnS/Mn on the structure, optical, and electric properties of PVC polymer. *Polymers*, 15(9), 2091
- [42] Rajendran, S., & Uma, T. (2000). Effect of ZrO<sub>2</sub> on conductivity of PVC-PMMA-LiBF<sub>4</sub>- DBP polymer electrolytes. *Bulletin of Materials Science*, 23(1), 31-34
- [43] Heiba, Z. K., El-naggar, A. M., Kamal, A. M., Abd-Elkader, O. H., & Mohamed, M. B. (2023). Extraction and studies of optoelectrical parameters of PVC/ZnO. 9M0. 1S (M: Co, Fe, Mn, V) films. *Optical Materials*, 143, 114282.

- [44] Ramesh, S., & Chao, L. Z. (2010). Investigation of dibutyl phthalate as plasticizer on poly(methyl methacrylate)–lithium tetraborate based polymer electrolytes. *Ionics*, 17(1), 29–34.
- [45] Rhoo, H.-J., Kim, H.-T., Park, J.-K. and Hwang, T.-S. (1997) Ionic conduction in plasticized PVC/PMMA blend polymer electrolytes. *Electrochimica Acta*, 42(10), 1571-1579.
- [46] Barkhordari, A., Altindal, Ş., Pirgholi-Givi, G., Mashayekhi, H., Özçelik, S., & Azizian-Kalanderagh, Y. (2023). The influence of PVC and (PVC: SnS) interfacial polymer layers on the electric and dielectric properties of Au/n-Si structure. *Silicon*, 15(2), 855-865.
- [47] Pradhan, D. K., Choudhary, R.N.P. and Samantaray B. K. (2008). Studies of structural, thermal and electrical behavior of polymer nanocomposite electrolytes. *Express Polymer Letters*, 2, 630-638
- [48] Singh, P.K., Kim, K.W. & Rhee, H.W. (2009). Development and characterization of ionic liquid doped solid polymer electrolyte membranes for better efficiency. *Synthetic Metals*, 159, 1538–1541.